Available online at www.sciencedirect.com
ScienceDirect
Journal of the European Ceramic Society 26 (2006) 3139–3143
www.elsevier.com/locate/jeurceramsoc

Diffusion of niobium in yttria-stabilized zirconia and in titania-doped yttria-stabilized zirconia polycrystalline materials

K. Kowalski [a,*], A. Bernasik [b], J. Camra [c], M. Radecka [d], J. Jedliński [c,d]

[a] *Department of Materials Science and Analysis, Faculty of Metallurgy and Materials Science, AGH-University of Science and Technology, Al. Mickiewicza 30, PL-30-059 Kraków, Poland*
[b] *Faculty of Physics and Applied Computer Science, AGH-University of Science and Technology, Al. Mickiewicza 30, PL-30-059 Kraków, Poland*
[c] *Regional Laboratory of Physicochemical Analysis and Structural Research, Jagellonian University, Ul. Ingardena 3, PL-30-060 Kraków, Poland*
[d] *Faculty of Materials Science and Ceramics, AGH-University of Science and Technology, Al. Mickiewicza 30, PL-30-059 Kraków, Poland*

Received 2 July 2005; received in revised form 27 September 2005; accepted 8 October 2005
Available online 21 November 2005

Abstract

Bulk and grain boundary diffusion of Nb^{5+} cations in yttria-stabilized zirconia (YSZ, 8 mol% Y_2O_3–92 mol% ZrO_2) and in titania-doped yttria-stabilized zirconia (Ti–YSZ, 5 mol% TiO_2–8 mol% Y_2O_3–87 mol% ZrO_2) was studied in air in the temperature range from 900 to 1300 °C. Experiments were performed in the B-type kinetic region. Diffusion profiles were determined using the secondary ion mass spectrometry (SIMS). The temperature dependencies of the bulk diffusion coefficient D and the grain boundary diffusion parameter $D'\delta s$ for both the materials were calculated. The activation energies of these transport processes in YSZ amounts to 258 and 226 kJ mol^{-1}, respectively, and 232 and 114 kJ mol^{-1} in Ti–YSZ. The results were compared to the diffusion data of other cations previously obtained for the same material.

Keywords: Grain boundaries; Diffusion; ZrO_2; Nb; Grain boundary diffusion

1. Introduction

Yttria-stabilized cubic zirconia (YSZ) ceramic material is used in many applications as a solid state electrolyte (e.g. solid oxide fuel cells (SOFC), oxygen sensors or oxygen membranes). Electrolyte properties of this material at elevated temperatures are governed by the anion transport in defected oxygen sublattice but its stability during working depends mainly on the slow cation transport. It controls such processes as sintering, creep, recrystallization, migration of dopants and impurities, etc. Many solid electrolyte devices are built as thin film systems consisted of different oxides or metals (alloys) and oxides. Main degradation process in such devices occurs by the interdiffusion of cations from adjoining layers. In this case, grain boundary diffusion plays very important role, which predominates over the lattice diffusion at 600–1000 °C, where the solid electrolytes based on YSZ usually operate.

Bulk (lattice) diffusion and, particularly, grain boundary diffusion in YSZ still remain not well-studied problems. Sparse works on the diffusion in cubic zirconia stabilized with different oxides, which were done before the year 2000, were reviewed in our previous articles.[1–3] The majority of these investigations were made in very high temperatures and by use of indirect experimental methods. Since that time some new papers have appeared.[4–13] Kilo et al.[4–7] investigated diffusion of Zr and Y in YSZ monocrystal and diffusion of Zr and Ca in calcia-stabilized zirconia (CSZ) single crystal with different content of stabilizers. Simultaneous bulk diffusion of lanthanide elements in monocrystals was studied by Weber et al.[8] for YSZ, by Taylor et al.[9] for YSZ, CSZ and scandia-stabilized zirconia (ScSZ) and by Kilo et al.[10] for CSZ and YSZ. The aim of these works was to find a correlation between ionic radius and cation diffusion in differently stabilized zirconia. Lakki et al.[11] investigated diffusion in polycrystalline YSZ but only the bulk diffusion of Zr was reported. Both, grain boundary and bulk diffusion were studied in the work of Bak et al.[12] for Mg migration in polycrystalline YSZ and in the work of Taylor et al.[13] for Zr diffusion in polycrystalline ScSZ.

* Corresponding author. Tel.: +48 12 617 27 16; fax: +48 12 634 30 70.
E-mail address: kowalski@metal.agh.edu.pl (K. Kowalski).

0955-2219/$ – see front matter © 2005 Elsevier Ltd. All rights reserved.
doi:10.1016/j.jeurceramsoc.2005.10.004

During last few years the secondary ion mass spectrometry (SIMS) technique became a major tool for investigations of diffusion in zirconia ceramics.[1–6,8–13] This method has the possibility to analyze isotopes that is useful for studying the self-diffusion by isotope labeling. Moreover, diffusion profiles can be determined precisely at very short distances what is important for observing the migration of slow cations in zirconia.

The present work is a continuation of the earlier investigations[1–3] when the diffusion parameters of Ti^{4+} and Ca^{2+} in bulk and in grain boundaries were determined for cubic YSZ. This time the Nb^{5+} cation was chosen for diffusion studies. Besides, exactly the same YSZ material as previously, also titania-doped yttria-stabilized zirconia (Ti–YSZ) ceramics was used for diffusion experiments. Ti–YSZ is a promising material for SOFC electrodes as a mixed oxygen ion-electron conductor at elevated temperatures under reduced oxygen partial pressure.[14]

2. Experimental

The YSZ samples (8 mol% Y_2O_3–92 mol% ZrO_2) used in this work were the same as in the previous diffusion studies.[1–2] They were prepared by sintering at 1700 °C of the pressed fine-grained oxide powders. The powders were obtained by the coprecipitation of zirconium and yttrium chlorides and their subsequent calcination. The Ti–YSZ specimens (5 mol% TiO_2–8 mol% Y_2O_3–87 mol% ZrO_2) were prepared using the same procedure and the same chlorides with only addition of the titanium chloride. In this case the temperature of sintering was 1500 °C. The sample preparation is described in details in the earlier articles.[1–2,15] Both zirconia materials were compact with densities higher than 99% of the theoretical value. Total amount of impurities did not exceed 0.1 wt%. The grain size was in the range 10–20 μm. X-ray diffraction analyses (XRD) revealed the cubic zirconia phase only.

Thin films of Nb_2O_5 were deposited on the polished surface of the samples by RF plasma sputtering from the very pure Nb target in an $Ar + O_2$ gas mixture at low pressure. The films were amorphous. Their thickness was about 30 nm. The oxidation state of Nb^{5+} ions was confirmed by the X-ray photoelectron spectroscopy (XPS) analysis.

The mean concentration depth profiles and the lateral distribution maps of niobium were determined by the SIMS method. The analyzer was equipped with the double lens liquid gallium ion beam gun (by FEI Company) and the quadrupole mass spectrometer (by Balzers). The energy of the Ga^+ ions equaled to 25 keV. Depths of the sputtered craters were measured with a profilometer. Then, they were used to calculate the sputtering rate. This rate was controlled by the sputter area, which was usually from 50 μm × 50 μm to 100 μm × 100 μm and by the primary ion current, which reached 2 nA at maximum. Undesirable crater edge effects were minimized by analyzing exclusively the ions coming from the central 40% of the crater area by use of an electronic gate. Charging effects were eliminated by applying the electron flood gun, with the energy of about 250 eV.

Diffusion experiments were done in air at 900, 1000, 1100, 1200 and 1300 °C for 48, 24, 6, 3 and 1 h, respectively. The temperature stability was within the range of ±2 °C. No further sintering or grain size variations were observed.

3. Results

Diffusion profiles were determined by measuring the signal intensities of four isotopes: ^{89}Y, ^{90}Zr, ^{93}Nb and ^{94}Zr on sputtering. As the crater area was large compared to the grain size, these intensities were proportional to the mean concentration of monitored isotopes. The experimental conditions fulfilled the requirements of the B-type kinetic regime.[16] In the regime B the mean concentration profile of the diffusing tracer consists of two parts. If the initial tracer layer is very thin (i.e. instantaneous source), like in the present work, then from the first part of the profile one can calculate the bulk diffusion coefficient D, according to the following formula:[16]

$$D = -\left(4t\frac{\partial \ln \bar{c}}{\partial x^2}\right)^{-1} \quad (1)$$

where t is diffusion time and $\bar{c}$ the mean concentration of the tracer at depth x.

From the second part of the profile one can determine the grain boundary diffusion parameter $D'\delta s$ (where D' is a grain boundary diffusion coefficient, δ the grain boundary width and s is the segregation factor of the tracer at the grain boundaries), according to the subsequent expression:[16]

$$D'\delta s = 0.66\left(-\frac{\partial \ln \bar{c}}{\partial x^{6/5}}\right)^{-5/3}\left(\frac{4D}{t}\right)^{1/2} \quad (2)$$

Fig. 1 shows the typical diffusion profile of Nb that consists of two well distinguished parts. The data are presented in the form of the secondary ion intensity ratio of ^{93}Nb to ^{90}Zr isotopes. This ratio can be considered as proportional to the concentration of niobium if this concentration is low. The dots represent experimental points and the solid lines are theoretical curves fitted using Eqs. (1) and (2) by the least-square method. Fitting procedure allowed to determine the values of D and $D'\delta s$ for each profile. Fig. 2 illustrates the lateral distribution of Nb for diffusion in Ti–YSZ at 1300 °C for 1 h at two depths. This figure confirms that it is justified to consider the Nb diffusion in this sample in terms of the B-type kinetic region. The

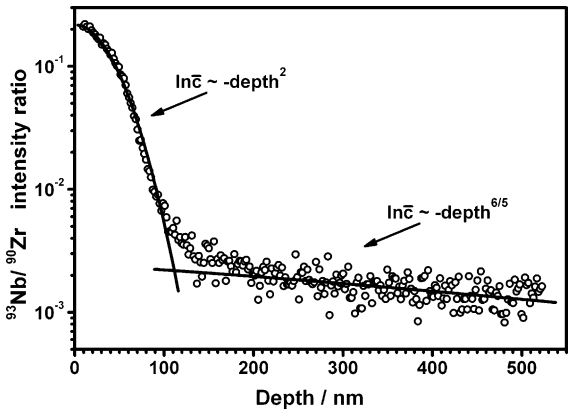

Fig. 1. Depth profile obtained for Nb diffusion in Ti–YSZ at 1000 °C for 24 h.

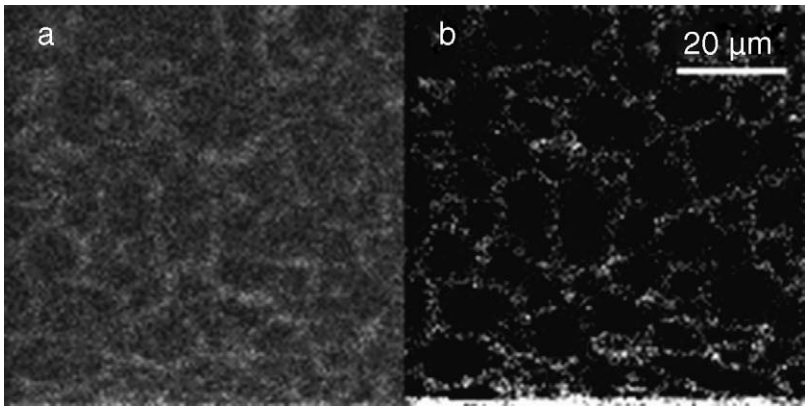

Fig. 2. Lateral distribution of ^{89}Nb at depth of (a) 85 nm and (b) 260 nm for diffusion in Ti–YSZ at 1300 °C for 1 h.

map presented in Fig. 2a, taken near surface, reveals inside the grains the presence of Nb that diffused directly from the sample surface. On the contrary, the map in Fig. 2b, taken much deeper, shows the presence of Nb only near the grain boundaries what is in agreement with the requirements of the regime B.[16] The SIMS maps of the ^{89}Y, ^{90}Zr and ^{48}Ti (not shown here) demonstrated the uniform lateral distribution of these isotopes.

All values of the bulk diffusion coefficients and the grain boundary diffusion parameters of Nb, determined from the diffusion profiles, for YSZ and Ti–YSZ are presented as Arrhenius plots in Fig. 3a and b, respectively. Their dependencies on temperature are expressed by the following relationships:

$$D_{\mathrm{Nb/YSZ}} = 2.6(\pm 3.6)10^{-10} \times \exp\left(\frac{-258(\pm 16)\,\mathrm{kJ\,mol^{-1}}}{RT}\right) \quad \mathrm{m^2 s^{-1}} \tag{3}$$

$$D'\delta s_{\mathrm{Nb/YSZ}} = 3.8(\pm 8.7) \times 10^{-17} \times \exp\left(\frac{-226(\pm 26)\,\mathrm{kJ\,mol^{-1}}}{RT}\right) \quad \mathrm{m^3 s^{-1}} \tag{4}$$

$$D_{\mathrm{Nb/Ti-YSZ}} = 2.2(\pm 1.1)10^{-11} \times \exp\left(\frac{-232(\pm 6)\,\mathrm{kJ\,mol^{-1}}}{RT}\right) \quad \mathrm{m^2 s^{-1}} \tag{5}$$

$$D'\delta s_{\mathrm{Nb/Ti-YSZ}} = 4.3(\pm 6.1) \times 10^{-21} \times \exp\left(\frac{-114(\pm 17)\,\mathrm{kJ\,mol^{-1}}}{RT}\right) \quad \mathrm{m^3 s^{-1}} \tag{6}$$

where T is absolute temperature and R the gas constant. Values in brackets are standard deviations of the determined values.

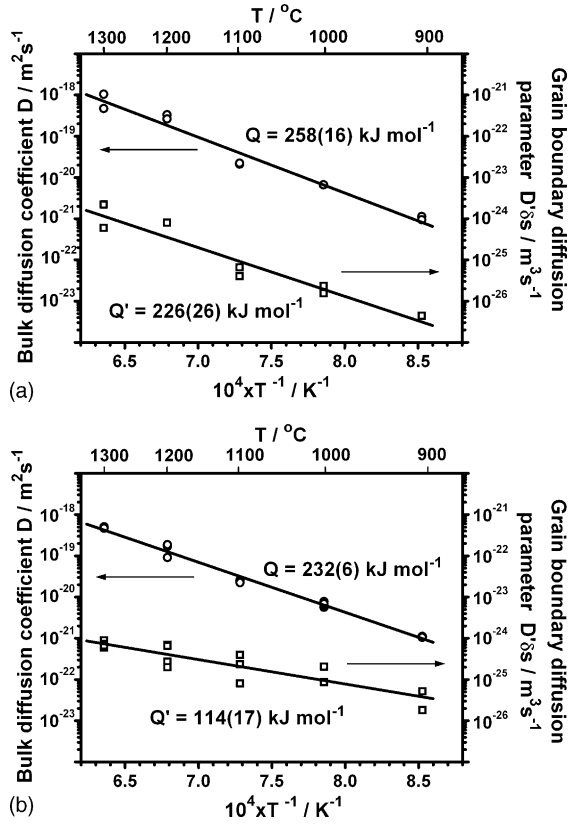

Fig. 3. Arrhenius plots of bulk and grain boundary diffusion data for Nb^{5+}: (a) in YSZ and (b) in Ti–YSZ.

4. Discussion

Comparison of the Nb^{5+} diffusion data with those of Ti^{4+} and Ca^{2+}, which were obtained for the same zirconia material,[1,2] is presented in Fig. 4. In the investigated temperature region the bulk diffusion coefficients for Nb^{5+} in YSZ have the values of the order of those for Ti^{4+} and Ca^{2+}; however, the activation energy equal to $258 \pm 16\,\mathrm{kJ\,mol^{-1}}$ for Nb^{5+} is distinctly lower than that for Ti^{4+} ($505 \pm 32\,\mathrm{kJ\,mol^{-1}}$) and Ca^{2+} ($333 \pm 25\,\mathrm{kJ\,mol^{-1}}$). The errors of the activation energies in this section should be understood as standard deviations of the calculated values by the least-square method from Arrhenius plots of the experimentally determined diffusion coefficients.

Recently, Kilo et al.[17] applied computer modeling technique to calculate the bulk diffusion activation energies for

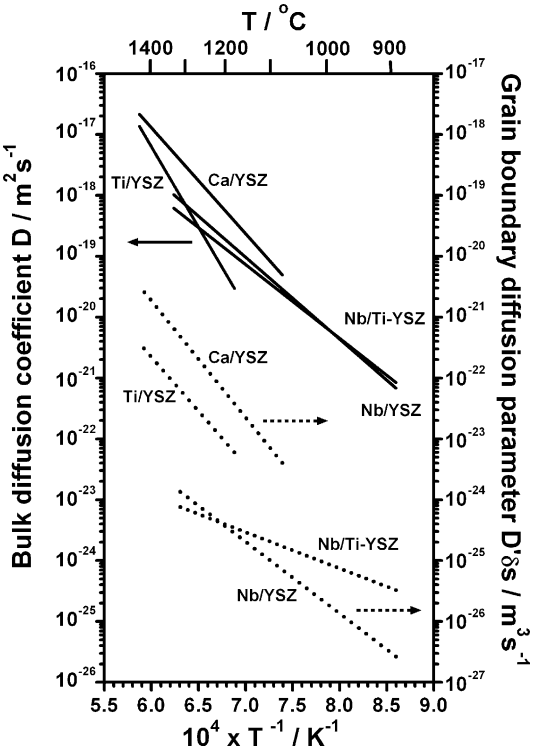

Fig. 4. Comparison of the Nb^{5+} diffusion data obtained in this work with the previous[1,2] results for Ti^{4+} and Ca^{2+} diffusion in the same zirconia material. Solid and dot lines correspond to the bulk diffusion coefficient D and to the grain boundary diffusion parameter $D'\delta$s, respectively.

some cations: Ca^{2+}, Y^{3+}, Ce^{3+}, Ce^{4+}, Zr^{4+} and Nb^{5+} in pure cubic ZrO_2. These cations have different charges and sizes. The authors found that the activation energy of diffusion increased with the charge density of cations following a smooth curve. The charge density of cation was defined as the ratio of its charge to its radius cubed. Thus, for the diffusion of Ca^{2+}, having the charge density equal to 1.42×10^{-6} e/pm^3 (e is an elementary charge); the calculated activation energy was 3.06 eV ≈ 295 kJ mol^{-1}, which was the lowest energy in that study. The highest activation energy (6.69 eV ≈ 646 kJ mol^{-1}) was found for the diffusion of Nb^{5+}, which has the charge density equal to 12.34×10^{-6} e/pm^3. It must be noted that the ion migration pathway was a straight line between adjacent ion sites for Ca^{2+} migration, while for Nb^{5+} it was a nonlinear pathway. On the assumption that the pathway for Nb^{5+} migration was also a straight-line, much higher value of the activation energy was found (13.53 eV ≈ 1306 kJ mol^{-1}), but this result was rejected as energetically less favorable.

The experimental value of the activation energy of the Nb^{5+} bulk diffusion, determined in the present work, is 2.5 times lower than that theoretically calculated by Kilo et al.[17] Moreover, the experimental value of the activation energy for Ti^{4+} equal to 505 kJ mol^{-1} (≈5.25 eV) is also lower than that estimated from the model of Kilo et al. The activation energy of Ti^{4+} diffusion was not calculated, but considering its charge density (9.87×10^{-6} e/pm^3) it should have a value of about 6.4 eV (≈618 kJ mol^{-1}) according to that model. The discrepancies between experimental and theoretical results probably may be explained either by the fact that in computer modeling only the pure ZrO_2 cubic phase was considered and the influence of stabilizers was neglected, or by the fact that some other assumptions of the migration model were inadequate. Contrary to the experimental data for Nb^{5+} and Ti^{4+}, the experimental value of the activation energy of Ca^{2+} diffusion in YSZ is close to the theoretically calculated value by Kilo et al.

The Nb^{5+} bulk diffusion coefficients determined for the titania-doped YSZ are very close to those for YSZ (see Fig. 4). The activation energy for Ti–YSZ is almost the same (232±6 kJ mol^{-1}) as for YSZ within the range of experimental error. Ti^{4+} cations substitute Zr^{4+} ions in the lattice of the cubic zirconia. Because the Ti^{4+} cations are smaller than the Zr^{4+} ones (74 pm compared to 84 pm, respectively), the lattice parameter slightly decreases with increasing content of titania.[14] Moreover, titanium cations prefer coordination of 6, which is characteristic for rutile than of 8, which is characteristic for cubic zirconia. Therefore, Ti^{4+} ions attract oxygen vacancies and tend to form associated pairs with them. This attraction causes the diminution of the oxygen ion conductivity. When the titania concentration reaches about 10 mol% then the tetragonal phase appears.[14] From the diffusion data for Nb^{5+} results that the TiO_2-doping at the level of 5 mol% has no significant impact on the bulk diffusion character in the cation sublattice.

As in the bulk, the activation energy of the grain boundary diffusion of Nb^{5+} in YSZ (226 ± 26 kJ mol^{-1}) is lower than those obtained for the same YSZ material for Ti^{4+} (340 ± 39 kJ mol^{-1}) and Ca^{2+} (367 ± 46 kJ mol^{-1}). Also the absolute values of the grain boundary diffusion parameters are lower than those for Ti^{4+} and Ca^{2+} (see Fig. 4).

Contrary to the bulk diffusion process, the titania doping has a considerable effect on the grain boundary diffusion since the activation energy of the Nb^{5+} grain boundary diffusion in Ti–YSZ is about two times lower than in YSZ and amounts to 114 ± 17 kJ mol^{-1}. In consequence, also the ratio of activation energies of bulk diffusion to grain boundary diffusion is different for both the systems. This ratio is equal to 0.88 ± 0.16 for YSZ and 0.49 ± 0.09 for Ti–YSZ. The difference may be caused by different structure and/or chemical composition of grain boundaries in both the materials. There is no experimental data to confirm this supposition; however, the surface segregation studies,[15] performed for the same ceramics, showed a small segregation effect of titanium at free surface in Ti–YSZ with a segregation factor of about 3–5 in the temperature range of 800–1400 °C. Similar effect is also probable at grain boundaries.

Assuming that the grain boundary width is of the order of 1 nm, what is generally approved in the literature,[12,13,16] and that the segregation factor for these tracers is less than 10; it is possible to estimate the grain boundary diffusion enhancement factor defined as the ratio D'/D. In the investigated temperature range the grain boundary enhancement factor for the Nb^{5+} diffusion is of the order of 10^4, while for Ti^{4+} and Ca^{2+} it is of the order of 10^5–10^6. For the Nb^{5+} diffusion in Ti–YSZ this factor changes from 10^4 at 900 °C to 10^5 at 1300 °C. Below 1200 °C the grain boundary diffusion is faster in Ti–YSZ, but above this temperature the relation is reversed.

5. Conclusions

The activation energy of the Nb^{5+} bulk diffusion in YSZ is lower than that of Ti^{4+} and Ca^{2+}, which were obtained for the same material.[1,2] This result is in discrepancy with the result of the theoretically determined activation energy of the Nb^{5+} migration in pure cubic ZrO_2 by Kilo et al.[17] The 5 mol% titania-doping in YSZ has no significant effect on the Nb^{5+} bulk diffusion character. The Nb^{5+} activation energy of the bulk diffusion in Ti–YSZ is very close to that in YSZ in the range of experimental error and the values of the diffusion coefficients are almost the same. Contrary to this, the TiO_2-doping has an important impact on the grain boundary diffusion. The activation energy of the grain boundary diffusion parameter $D'\delta$s in YSZ is two times greater than that for Ti–YSZ.

Acknowledgement

The Polish State Committee for Scientific Research financially supported this work.

References

1. Kowalski, K., Bernasik, A. and Sadowski, A., Bulk and grain boundary diffusion of titanium in yttria stabilized zirconia. *J. Eur. Ceram. Soc.*, 2000, **20**, 951–958.
2. Kowalski, K., Bernasik, A. and Sadowski, A., Diffusion of calcium in yttria fully stabilized zirconia ceramics. *J. Eur. Ceram. Soc.*, 2000, **20**, 2095–2100.
3. Kowalski, K., Bernasik, A., Sadowski, A. and Jedliński, J., Application of secondary ion mass spectrometry in the investigation of diffusion in ceramics. In *Mass and Charge Transport in Inorganic Materials. Fundamentals to Devices*, ed. P. Vincenzini and V. Buscaglia. Techna Srl, 2000, pp. 573–580.
4. Kilo, M., Borchardt, G., Lesage, B., Kaïtasow, O., Weber, S. and Scherrer, S., Cation transport in yttria stabilized cubic zirconia: ^{96}Zr tracer diffusion in $(Zr_xY_{1-x})O_{2-x/2}$ single crystals with $0.15 \leq x \leq 0.48$. *J. Eur. Ceram. Soc.*, 2000, **20**, 2069–2077.
5. Kilo, M., Weller, M., Borchardt, G., Damson, B., Weber, S. and Scherrer, S., Cation mobility in Y_2O_3- and CaO-stabilised ZrO_2 studied by tracer diffusion and mechanical spectroscopy. *Defect Diffusion Forum*, 2001, **194–199**, 1039–1044.
6. Kilo, M., Borchardt, G., Lesage, B., Weber, S., Scherrer, S., Schroeder, M. *et al.*, Y and Zr tracer diffusion in yttria-stabilized zirconia at temperatures between 1250 and 2000 K. *Key Engin. Mater.*, 2002, **206–213**, 601–604.
7. Kilo, M., Taylor, M. A., Argirusis, Ch., Borchardt, G., Lesage, B., Weber, S. *et al.*, Cation self-diffusion of ^{44}Ca, ^{88}Y and ^{96}Zr in single-crystalline calcia- and yttria-doped zirconia. *J. Appl. Phys.*, 2003, **94**, 7547–7552.
8. Weber, S., Scherrer, S., Scherrer, H., Kilo, M., Taylor, M. A. and Borchardt, G., SIMS analysis of multi-diffusion profiles of lanthanides in stabilized zirconias. *Appl. Surf. Sci*, 2003, **203–204**, 656–659.
9. Taylor, M. A., Argirusis, Ch., Kilo, M., Borchardt, G., Luther, K.-D. and Assmus, W., Correlation between ionic radius and cation diffusion in stabilised zirconia. *Solid State Ionics*, 2004, **173**, 51–56.
10. Kilo, M., Taylor, M. A., Argirusis, Ch. and Borchardt, G., Lanthanide transport in stabilized zirconias: Interrelation between ionic radius and diffusion coefficient. *J. Chem. Phys.*, 2004, **121**, 5482–5487.
11. Lakki, A., Herzog, R., Weller, M., Schubert, H., Reetz, C., Görke, O. *et al.*, Mechanical loss, creep, diffusion and ionic conductivity of ZrO_2-8 mol%Y_2O_3 polycrystals. *J. Eur. Ceram. Soc.*, 2000, **20**, 285–296.
12. Bak, T., Nowotny, J., Prince, K., Rekas, M. and Sorrell, C. C., Grain boundary diffusion of magnesium in zirconia. *J. Am. Ceram. Soc.*, 2002, **85**, 2244–2250.
13. Taylor, M. A., Kilo, M., Borchardt, G., Weber, S. and Scherrer, H., ^{96}Zr diffusion in polycrystalline scandia stabilized zirconia. *J. Eur. Ceram. Soc.*, 2005, **25**, 1591–1595.
14. Colomer, M. T. and Jurado, J. R., Structure, microstructure and mixed conduction of $[(ZrO_2)_{0.92}(Y_2O_3)_{0.08}]_{0.9}(TiO_2)_{0.1}$. *J. Solid State Chem.*, 2002, **165**, 79–88.
15. Bernasik, A., Kowalski, K. and Sadowski, A., Surface segregation in yttria stabilized zirconia by means of angle resolved X-ray photoelectron spectroscopy. *J. Phys. Chem. Solids*, 2002, **62**, 233–239.
16. Kaur, I. and Gust, W., *Fundamentals of Grain and Interface Boundary Diffusion*. Ziegler Press, Stuttgart, 1988, pp. 29–101.
17. Kilo, M., Jackson, R. A. and Borchardt, G., Computer modelling of ion migration in zirconia. *Philos. Mag.*, 2003, **83**, 3309–3325.